1 March 2001

ELSEVIER

Optics Communications 189 (2001) 87–96

OPTICS COMMUNICATIONS

www.elsevier.com/locate/optcom

Spatial periodicity enhanced superradiance from an optically dense two-level medium

Jamal T. Manassah [a,*], Irina Gladkova [b]

[a] HMS Technology Corporation, P.O. Box 592, New York, NY 10028-0005, USA
[b] Department of Computer Science, City College of New York, New York, NY 10031, USA

Received 27 September 2000; accepted 8 December 2000

Abstract

We show that, in an optically dense medium having an inverted active atom number density periodically distributed in space, it is possible, in a slab configuration, to enhance the forward–backward symmetric superradiance emission efficiency if the periodicity reciprocal lattice vector obeys a Bragg's-like condition for coupling the forward and backward components of the active atoms polarization. We also show that the burst of superradiant light is emitted, in this case, at an earlier time than that for a homogeneously distributed medium having the same average atomic number density. Furthermore, this burst's temporal duration is shown to be substantially shorter than that for the homogeneous active atoms distribution. © 2001 Published by Elsevier Science B.V.

Keywords: Superradiance; Optically dense material; Periodic doping

1. Introduction

As a result of the high value of the reflectivity at every point along the propagation path of a signal in an optically dense resonant two-level medium (i.e. $\alpha\lambda < 1$), both the forward and backward waves need to be included in the analysis of Maxwell equations for this problem. The simultaneous presence of the forward and backward waves in this resonant gas results into situations where resonator-like standing waves can develop in the system without the need for end mirrors; this situation can be realized when the pressure broadening in a gas substantially exceeds the Doppler broadening, hence the name "pressure-induced resonators". In particular, we have previously shown [1–3] that, in the superradiant regime [4], an inverted system of such resonant atoms radiates such that the atomic polarization and the total field are eigenfunctions of the spatial inversion operator with respect to the center of the slab, for sample's length in, what we called, the symmetric sectors, and that an asymmetric transition domain separates two consecutive symmetric sectors with opposite parity eigenvalues. We have also found that, in the symmetric sectors, the electromagnetic field distributions are similar to those found in a slab resonant cavity, and that the forward and backward emission fluxes are equal.

In this paper, we investigate the system's superradiance dynamics if the active atoms number density is periodically distributed. We show that,

* Corresponding author. Fax: +1-212-650-7185.
E-mail address: manassah@ees2cd.engr.ccny.cuny.edu (J.T. Manassah).

0030-4018/01/$ - see front matter © 2001 Published by Elsevier Science B.V.
PII: S0030-4018(01)00992-0

in the symmetric sectors, the superradiance emission efficiency can be further enhanced if the reciprocal lattice vector of the active atoms periodic distribution obeys a Bragg's-like condition for maximum coupling between the forward and backward components of the polarization (forward and backward components of polarization refer to those quantities that are the source terms for the forward and backward components of the generated electromagnetic field). Furthermore, we show that:

(i) the burst of superradiant light, in the above medium, is emitted at an earlier time than that in a homogeneously distributed active medium having the same average atomic number density, and that
(ii) the superradiant burst temporal duration is substantially shorter here than that associated with an active atom homogeneous distribution.

We solve the problem numerically by integrating the coupled Maxwell–Bloch integro-differential coupled equations.

2. Maxwell–Bloch equations

The physical system that we analyze here is that of a passive dielectric medium doped with active atoms. In this atomic/dielectric medium system, the total polarization consists of the sum of the linear polarization due to the embedding dielectric medium plus the resonant polarization due to the two-level atomic system:

$$P = P_{\mathrm{NR}} + P_{\mathrm{R}} \tag{1}$$

The linear polarization P_{NR} (where the subscript NR stands for non-resonant, and R for resonant) is given by:

$$P_{\mathrm{NR}} = \alpha\varepsilon_0 E_{\mathrm{L}} \tag{2}$$

where α is the medium linear susceptibility, and the local (Lorentz) field E_{L} is given by [5]:

$$E_{\mathrm{L}} = E + P/3\varepsilon_0 \tag{3}$$

and where E is the Maxwell (macroscopic) field.

Using Eqs. (1)–(3), the total polarization can be written as [3,6]:

$$P = \frac{\alpha\varepsilon_0 E}{1-\frac{1}{3}\alpha} + \frac{P_{\mathrm{R}}}{1-\frac{1}{3}\alpha} \tag{4}$$

where P_{R} is obtained from Bloch equations, evaluated with the local field, and not the Maxwell field.

The above quantities can be directly related to the more familiar cases and quantities, through an examination of Eq. (4). For example, in the absence of the embedding dielectric medium, we obtain the atoms in vacuum result:

$$E_{\mathrm{L}} = E + \frac{P_{\mathrm{R}}}{3\varepsilon_0} \tag{5}$$

and in the absence of resonant medium, we obtain the Lorentz result:

$$E_{\mathrm{L}} = E + \frac{1}{3}\frac{\alpha E}{1-\frac{1}{3}\alpha} \tag{6}$$

which, of course, leads to the Clausius–Mosetti equation:

$$\frac{\varepsilon_{\mathrm{r}}-1}{\varepsilon_{\mathrm{r}}+2} = \frac{1}{3}\alpha$$

or

$$\varepsilon_{\mathrm{r}} = n_{\mathrm{r}}^2 = \frac{1+2\alpha/3}{1-\alpha/3} \tag{7}$$

where n_{r} is the passive dielectric's index of refraction which we assume here to be real. (The Kramer–Kronig relations, derived only on the assumption of causality, require that $\mathrm{Im}(n_{\mathrm{r}}) \neq 0$, however, we will work in the spectral regime where this contribution can be neglected over the propagation lengths under consideration.)

The dynamics of the interaction of the electromagnetic field with the ensemble of active two-level atom system is described by Bloch equations. If we neglect the counter-rotating term in the Hamiltonian, i.e. replacing the electromagnetic real field $(E\mathrm{e}^{-\mathrm{i}\omega_{\mathrm{c}}t} + E^*\mathrm{e}^{+\mathrm{i}\omega_{\mathrm{c}}t})$ by $E\mathrm{e}^{-\mathrm{i}\omega_{\mathrm{c}}t}$, where ω_{c} is the carrier frequency, Bloch equations reduce to:

$$\frac{\partial\chi}{\partial U} = -[\mathrm{i}[(\overline{\Omega}_0 - \overline{\Omega}_{\mathrm{c}}) + \overline{\Delta}] + \overline{\gamma}_2]\chi + \frac{\mathrm{i}n\phi_{\mathrm{L}}}{2} \tag{8}$$

$$\frac{\partial n}{\partial U} = -\mathrm{i}[\chi^*\phi_{\mathrm{L}} - \chi\phi_{\mathrm{L}}^*] + \overline{\gamma}_1(1-n) \tag{9}$$

where we are normalizing the dynamical variables and coordinates as follows:

$$\phi = \frac{dET_2^*}{\hbar}; \qquad \chi = \frac{p}{d}; \qquad U = \frac{t}{T_2^*};$$
$$\overline{\Delta} = \Delta T_2^*; \qquad \overline{\gamma}_{(1,2)} = \gamma_{(1,2)} T_2^*; \qquad \overline{\Omega}_{(0,c)} = \omega_{(0,c)} T_2^*$$

p is the x–y components of the Bloch vector, $p = p_x + \mathrm{i}p_y$, n is the population difference between the ground and excited states, ω_0 is the active atom resonant frequency, γ_1 and γ_2 are the longitudinal and transverse decay rates, d is the atomic transition dipole moment, T_2^* is the inhomogeneous dephasing time, and Δ is the detuning of a particular group of atoms in the ensemble from the single atom resonant frequency. The normalized local field ϕ_L is given by [3,6]:

$$\phi_L = \frac{1}{(1 - \frac{1}{3}\alpha)}\phi + \frac{8\beta}{3(1 - \frac{1}{3}\alpha)}\chi \tag{10}$$

where $\beta(\bar{z}) = \rho(\bar{z})d^2 T_2^*/8\hbar\varepsilon_0$ and $\rho(\bar{z})$ is the spatially dependent active atom number density. The normalized Lorentz shift [7,8], neglecting quantum corrections originating from the scattering amplitude due to collision between atoms and that are present in a gaseous medium, is then given for low excitation by $4\beta/3(1 - \alpha/3)$. The transverse relaxation decay rate consists of three components, the first being half the longitudinal relaxation constant; the second contribution is that due to the short range dipole–dipole interaction [7,8], which is very important here since the active atoms density is high in an optically dense medium; and the third contribution is that originating from the interaction of the active atoms with the different quantum modes of the dielectric medium and which may be controlled by cooling the dielectric medium, specifically:

$$\overline{\gamma}_2 = \frac{\overline{\gamma}_1}{2} + (1.16)(1.15)\left(\frac{2\pi}{3n_r^2}\right)\beta + \overline{\gamma}_T \tag{11}$$

Note that the additional factor of 1.16, in the second term, from the standard gas pressure broadened expression for the line width, corresponds to the off-the-mass shell correction to the scattering amplitude, which quantity should be used in the computation of the atomic self-energy when the active atoms are immobile and embedded in a dielectric. This is equivalent, as was shown in Ref. [8], to using the statistical theory results in computing the spectral broadening of the excited state due to the dipole–dipole interaction between as excited and a ground state atom.

Maxwell wave equation is given by:

$$\frac{\partial^2\phi}{\partial\bar{z}^2} - \varsigma^2\frac{\partial^2\phi}{\partial U^2} = \frac{8\beta\varsigma^2}{(1 + 2\alpha/3)}\left\langle \frac{\partial^2\chi}{\partial U^2}\right\rangle_{\overline{\Delta}} \tag{12}$$

where $\bar{z} = ((\omega_c n_r)/c)z$, $\varsigma = 1/\omega_c T_2^*$, and $\langle\chi\rangle_\Delta$ represents the normalized polarizability averaged over the inhomogeneous distribution, assumed here Gaussian, and given by:

$$g(\overline{\Delta}) = \frac{1}{\sqrt{2\pi}}\exp\left(-\frac{\overline{\Delta}^2}{2}\right) \tag{13}$$

To avoid the usual difficulties associated with solving a second-order differential equation (Eq. (12)) when the forward and backward waves are comparable in magnitude, we replace it by its equivalent integral equation form [9–12]:

$$\phi(\bar{z}, U) = \phi_{in}(\bar{z} = 0, U_{ret})\exp(\mathrm{i}\bar{z}) + \mathrm{i}\frac{4}{(1 + 2\alpha/3)} \times \int_0^{\bar{L}} \beta(\bar{z}')\exp(\mathrm{i}|\bar{z} - \bar{z}'|)\left\langle \chi\left(\bar{z}', U_{ret}, \overline{\Delta}\right)\right\rangle_\Delta \mathrm{d}\bar{z}' \tag{14}$$

where $\bar{L}$ is the normalized sample length, and the retarded normalized time is given, such that the space–time doublet is defined as follows:

$$(\bar{z}, U_{ret}) = (\bar{z}, U - \varsigma\bar{z}) \tag{15}$$

The mixed boundary and initial conditions for the problem are:

$$\phi_{in}(\bar{z} = 0, U) = \phi_{in}^0\exp\left(-\frac{U^2}{(\tau/T_2^*)^2}\right) \tag{16}$$

where $\phi_{in}^0 = \Sigma T_2^*/(\sqrt{\pi}\tau)$, and Σ is the incoming pulse area; and

$$\chi(\bar{z}, U = 0^-, \Delta) = 0 \tag{17}$$

$$n(\bar{z}, U = 0^-, \Delta) = -1 \tag{18}$$

for all $\bar{z} > 0$. $U = 0^-$ refers to the time prior to the incident external signal being switched on.

In our simulations, and in order to mimic the onset of superradiant emission, we shall assume that the atomic system is fully inverted and that the incoming pulse area is that associated with the rms value of the electromagnetic field vacuum

fluctuations [13–18], and such that its duration is longer than any of the relaxation times of the atomic system.

For the active atom spatial distribution, we assume that the profile is given by:

$$\beta(\bar{z}) = \beta_c(1 - \beta_m \cos(\beta_f \bar{z})) \tag{19}$$

where, in the usual convention, we refer to β_m as the amplitude of modulation and β_f as the modulation lattice vector.

3. Results

Fig. 1 shows previously obtained results [1,2]. Specifically, we illustrate the behavior of the atomic susceptibility for a homogeneous atomic distribution in what is called the symmetric sectors. Recall that in these sectors, the active atom polarization is an eigenfunction of the spatial parity operator, defined here as the inversion with respect to the center of the slab. Furthermore, recall that the eigenvalues associated with these

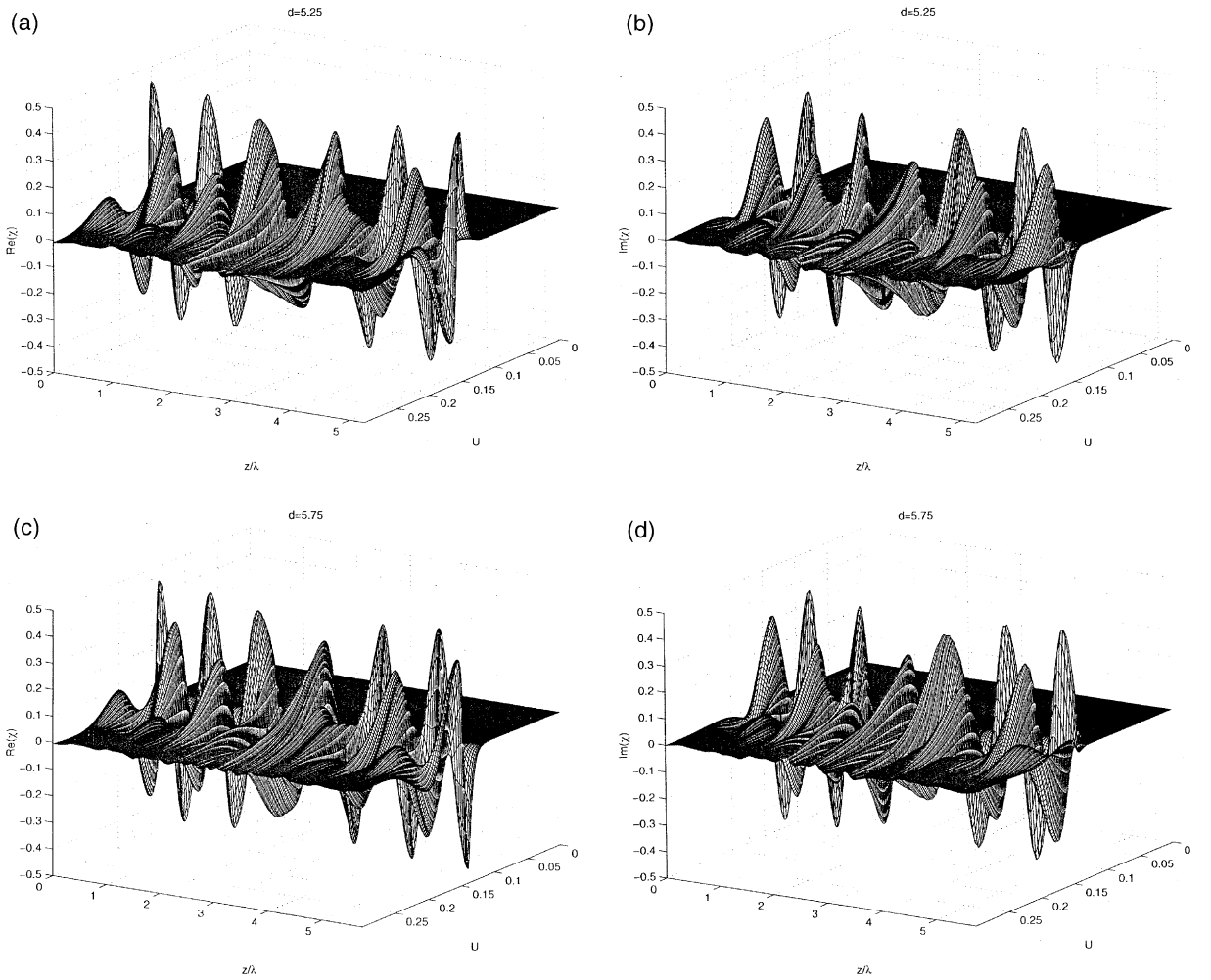

Fig. 1. The 3-D plot of the real and imaginary parts of the susceptibility of a system of initially fully inverted active atoms are plotted as function of the normalized position and time. $n_r = 1$; $\beta_c = 10$; $\beta_m = 0$; $\bar{\gamma}_1 = 1/25$; $\bar{\gamma}_T = 0$; $\varsigma = (10^6\ \pi)^{-1}$. (a) The real part of the susceptibility at $L = 5.25\lambda$; (b) the imaginary part of the susceptibility at $L = 5.25\lambda$; (c) the real part of the susceptibility at $L = 5.75\lambda$; (d) the imaginary part of the susceptibility at $L = 5.75\lambda$.

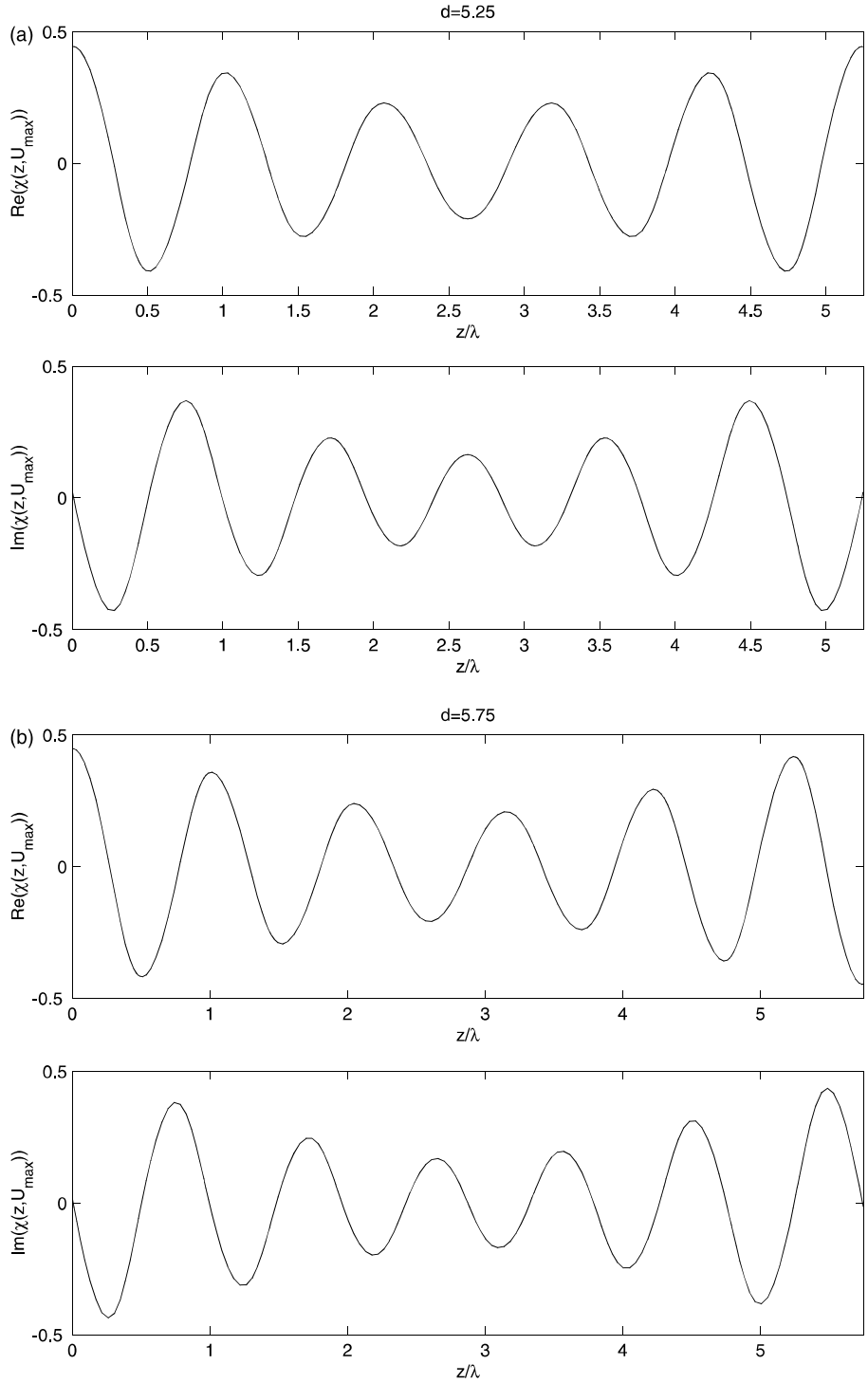

Fig. 2. The real and imaginary parts of the susceptibility are plotted as function of the normalized distance, at the time coordinate corresponding to the outgoing superradiant signal's peak. Same parameters as in Fig. 1.

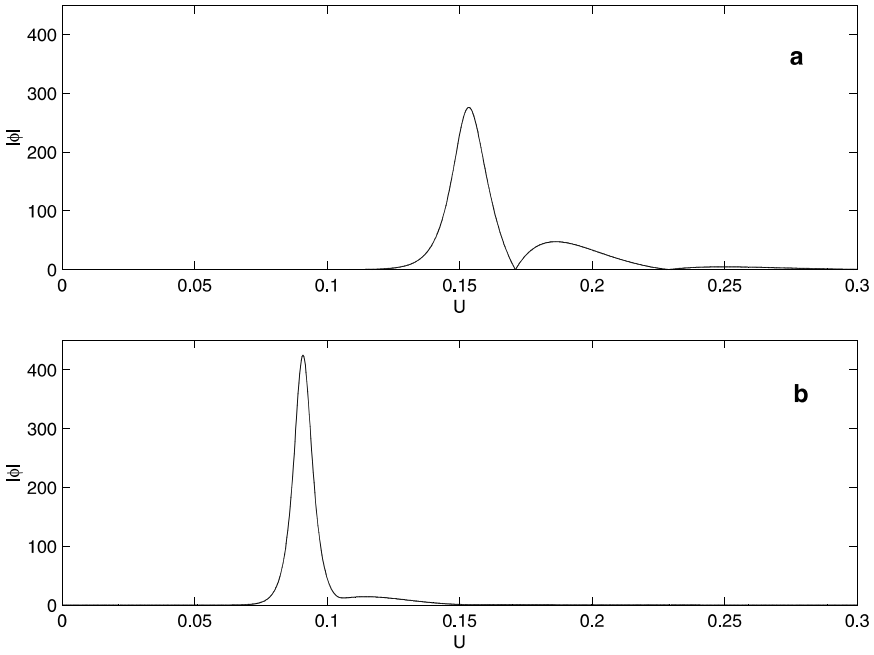

Fig. 3. The magnitude of the outgoing normalized field is plotted as function of the normalized time and compared for the cases of homogeneous and fully modulated active atoms distributions. $L = 5.25\lambda$; $n_r = 1$; $\beta_c = 10$; $\beta_f = 44/21$; $\bar{\gamma}_1 = 1/25$; $\bar{\gamma}_T = 0$; $\varsigma = (10^6\ \pi)^{-1}$ (a) $\beta_m = 0$; (b) $\beta_m = 1$.

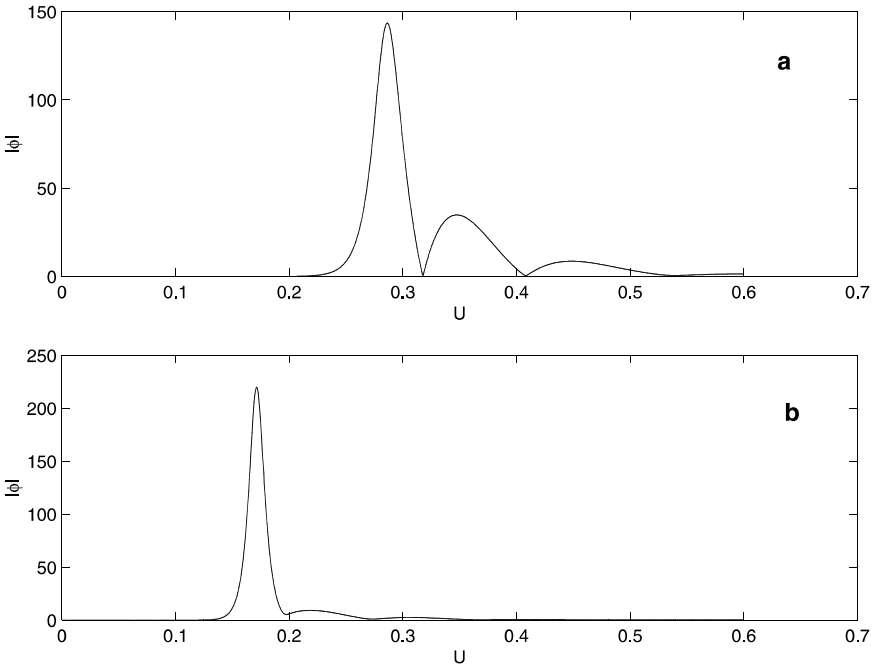

Fig. 4. Same as Fig. 3, with the following modifications: $L = 5.25\lambda/n_r$; $n_r = 2$. (a) $\beta_m = 0$; (b) $\beta_m = 1$.

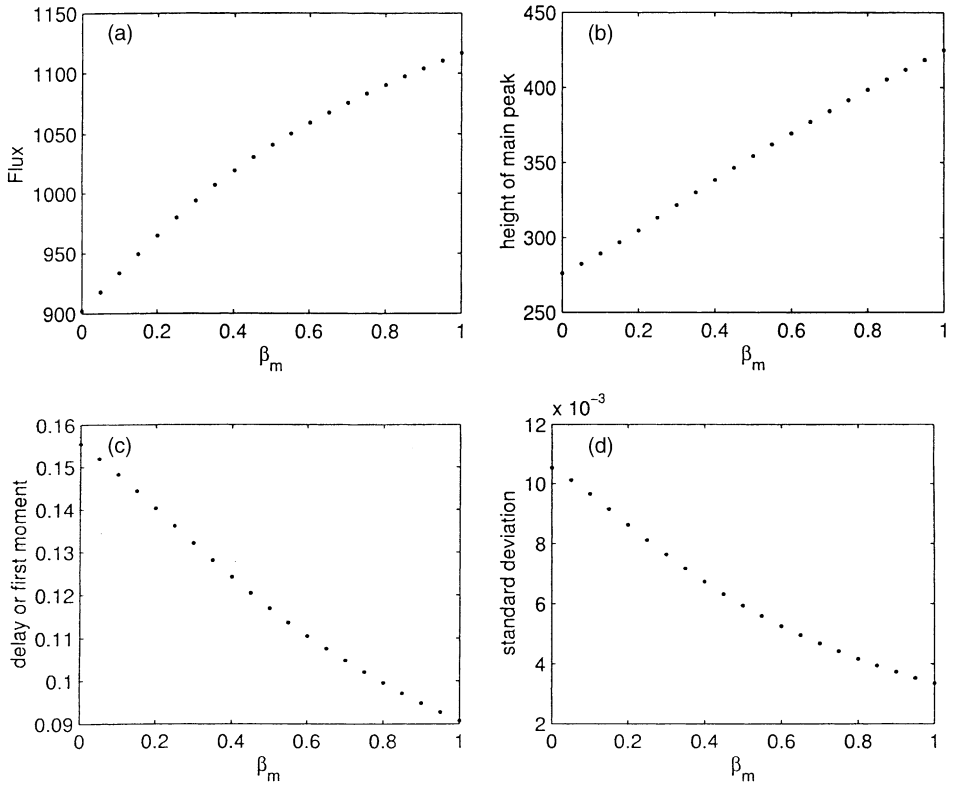

Fig. 5. (a) The flux of the outgoing normalized field; (b) height of the main peak of the magnitude of the outgoing field; (c) the first moment of the intensity of the outgoing field distribution; and (d) the second moment (standard deviation or width) of the intensity of the outgoing field distribution, are plotted as function of the depth of modulation, for an atomic distribution with a phased matched lattice vector. $L = 5.25\lambda$; $n_r = 1$; $\beta_c = 10$; $\beta_f = 44/21$; $\bar{\gamma}_1 = 1/25$; $\bar{\gamma}_T = 0$; $\varsigma = (10^6\ \pi)^{-1}$.

eigenfunctions alternate between the values ± 1, for consecutive symmetric sectors. These properties are more clearly shown in Fig. 2, where we plot the spatial dependence of the field temporal cross-section at the value of time corresponding to the position of the peak of the outgoing field distribution, for the two different parity states, shown in the previous figure. The standing wave structure observed is due to having at each point in the optically thick medium, the reflected electromagnetic wave being of comparable magnitude to the transmitted wave.

Having shown the standing wave feature in the homogeneous medium, the question arises as to whether by enhancing the coupling between the forward and backward components of the atomic polarization, we can increase the efficiency of the superradiance, shortens the time required for the onset of superradiance, and compress the duration of the superradiant burst, while maintaining the forward–backward symmetry in emission.

An analysis of Figs. 1 and 2 and other values of the sample length, lead us to the conclusion that if we select the sample length such that it is at the center of the symmetric sectors, i.e. for the values:

$$L = \frac{(2m+1)\lambda_0}{4n_r} \tag{20a}$$

where λ_0 is the radiation wavelength in vacuum, the values of β_f that would maintain the forward–backward symmetry in emission are given by:

$$\beta_f = \frac{4(m+1)}{(2m+1)} \quad \text{and} \quad \beta_f = \frac{4m}{(2m+1)} \tag{20b}$$

In Fig. 3, using the above obtained values of β_f, we show the temporal profile of the output field for

no and full modulation. As can be noted, all of the above three goals have been achieved. Furthermore, the temporal lobes, due to the Burnham–Chiao oscillations [19] have been greatly suppresed. In Fig. 4, we illustrate the case where even multiple lobes suppression is also achieved. The first value of β_f, as specified in Eq. (20b), gives slightly better results than those from the second value. We will use the value $\beta_f = 4(m+1)/(2m+1)$ in the following figures.

The effect of the depth of the modulation on the flux of either the transmitted (forward) or reflected (backward) output radiation, the height of the principal peak of the temporal profile, the superradiance delay (or first moment of the temporal distribution) and the standard deviation of the intensity temporal distribution (roughly the temporal width of the superradiant burst energy density) are plotted in Fig. 5. The main global features observed in Fig. 3 are shown, as expected, to follow a continuous and monotonic variation with an increase in the depth of modulation.

Next, we investigate the coherence length in this system when Eq. (20) is satisfied. We investigate the global features considered above for different length of the sample. In Fig. 6, we compare the main features of the superradiant burst for the homogeneous medium and for the fully modulated active atom distribution for different length of the sample. We observe that the features found previously hold for all values of length considered, hence we have long range coherence in the system, as would be expected. Furthermore, it should be noted that contrary to what happens in the homogeneous medium, where the number of Burnham–Chow oscillations increase with the length of

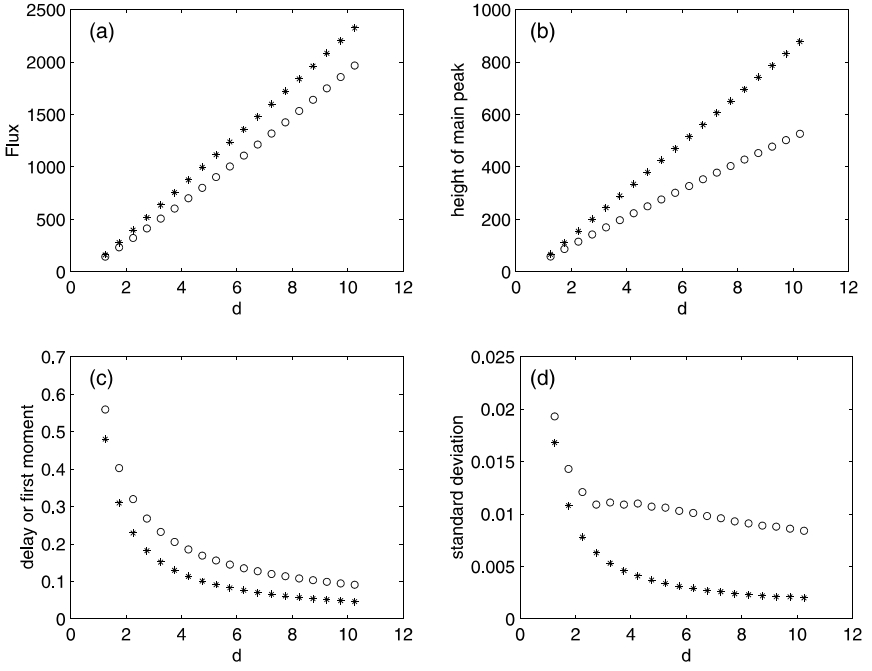

Fig. 6. (a) The flux of the outgoing normalized field; (b) height of the main peak of the magnitude of the outgoing field; (c) the first moment of the intensity of the outgoing field distribution; and (d) the second moment (standard deviation or width) of the intensity of the outgoing field distribution, are plotted as function of the sample length and compared for the zero and fully modulated distributions, for an atomic distribution with a phased matched lattice vector. (○) $\beta_m = 0$; (✱) $\beta_m = 1$. $L = ((2m+1)/4)\lambda$; $n_r = 1$; $\beta_c = 10$; $\beta_f = 4(m+1)/(2m+1)$; $\bar{\gamma}_1 = 1/25$; $\bar{\gamma}_T = 0$; $\varsigma = (10^6\ \pi)^{-1}$.

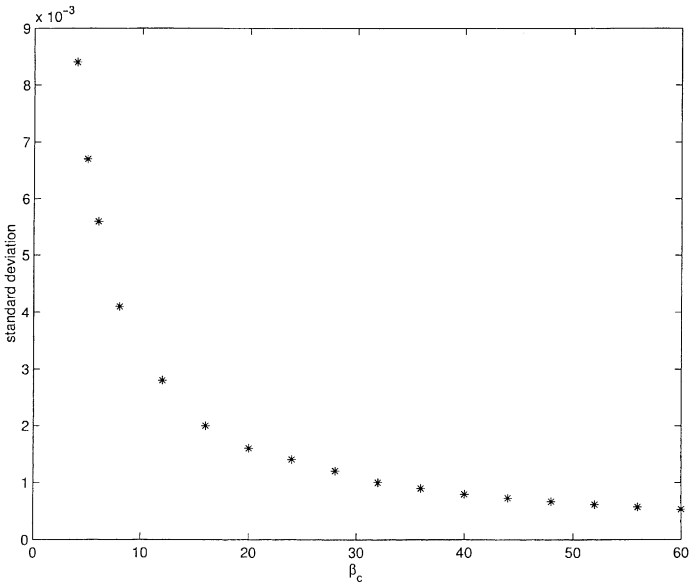

Fig. 7. The standard deviation of the temporal profile of the intensity of the outgoing field is plotted as function of β_c. $L = 5.25\lambda$; $n_r = 1$; $\beta_m = 10$; $\beta_f = 44/21$; $\bar{\gamma}_1 = 1/25$; $\bar{\gamma}_T = 0$; $\varsigma = (10^6\ \pi)^{-1}$.

the sample, in the present system these are attenuated, while the central lobe continues to compress.

Finally, we examine the dependence of the temporal width of the electromagnetic field intensity profile as function of β_c, the average value of β over a spatial period. As the atomic pressure broadening spectral width depends linearly on β, and as the spatial periodicity in the active atom density dampens the Burnham–Chiao oscillation and thus exclude any contribution that they may add to the intensity standard deviation, we should expect that the temporal width of the superradiant burst to decrease inversely with β_c. Fig. 7 shows the numerical results dependence. They follow closely the previous predictions.

4. Conclusion

In this paper, we investigated superradiant amplification from a system consisting of an ensemble of inverted resonant atoms in an optically dense medium with an active atom number density distribution that is spatially periodic. We showed that, with a judicious choice of the periodicity reciprocal lattice, we can maintain the forward–backward symmetry in emission while we vary qualitatively the shape, delay and flux of the superradiant burst. The resulting superradiant pulse can be made cleaner and leaner.

References

[1] J.T. Manassah, B. Gross, Opt. Commun. 143 (1997) 329.
[2] J.T. Manassah, B. Gross, Opt. Exp. 1 (1997) 141.
[3] J.T. Manassah, B. Gross, Opt. Commun. 155 (1998) 213.
[4] R.H. Dicke, Phys. Rev. 93 (1954) 99.
[5] H.A. Lorentz, The Theory of Electrons, Dover, New York, 1952.
[6] M.E. Crenshaw, C.M. Bowden, Phys. Rev. A 53 (1996) 1139.
[7] R. Friedberg, S.R. Hartmann, J.T. Manassah, Phys. Rep. C 7 (1973) 101.
[8] J.T. Manassah, Phys. Rep. 101 (1983) 359.
[9] V. Malyshev, E.C. Jarque, J. Opt. Soc. Am. 12 (1995) 1868.
[10] M.G. Benedict, E.D. Trifonov, Phys. Rev. 38 (1988) 2854.
[11] M.G. Benedict, V.A. Malyshev, E.D. Trifonov, I. Zaitsev, Phys. Rev. 43 (1991) 3854.
[12] J.T. Manassah, B. Gross, Opt. Commun. 131 (1996) 408.
[13] J.C. MacGillivray, M.S. Feld, Phys. Rev. A 14 (1976) 1169.
[14] J.C. MacGillivray, M.S. Feld, Phys. Rev. A 23 (1981) 1334.

[15] R. Bonifacio, L.A. Lugiato, Phys. Rev. A 11 (1975) 1507.
[16] R. Bonifacio, L.A. Lugiato, Phys. Rev. A 12 (1975) 587.
[17] R. Glauber, F. Haake, Phys. Lett. 68A (1978) 29.
[18] D. Polder, M.F.H. Schuurmans, Q.H.V. Vrehen, Phys. Rev. A 19 (1979) 1192.
[19] D.C. Burnham, R.Y. Chiao, Phys. Rev. 188 (1969) 667.